Boundary-induced spatiotemporal complex patterns in excitable systems

Olga Nekhamkina and Moshe Sheintuch

Department of Chemical Engineering, Technion, Israel Institute of Technology, Haifa 32000, Israel
(Received 31 October 2005; revised manuscript received 20 April 2006; published 28 June 2006)

We show that inhomogeneous boundary conditions (BCs) in a distributed reaction-diffusion excitable system are a natural source of permanent perturbations that can induce wave trains, which can be characterized as mixed-mode temporal oscillations and, when a parameter is varied, admit a period-adding bifurcation. To that end we analyze: a pair of coupled excitable and oscillatory cells, a distributed FitzHugh-Nagumo model, and a distributed five-variable model that describes CO catalytic oxidation. The obtained results account for the recently reported experimental observations of mixed-mode oscillations showing a period-adding bifurcation during CO oxidation on a disk-shaped catalytic cloth with imposed cold temperature BC.

While pattern formation in unbounded or large [subject to no-flux boundary conditions (BCs)] reaction-diffusion (RD) systems have been extensively investigated [1–4], relatively little attention has been paid to RD systems subject to Dirichlet or mixed BCs. Boundary effects are important in most catalytic systems (see review [5]), in cardiac [6] as well as in many other systems. Pulse waves can be reflected from the no-flux boundary in excitable RD systems [7]. The inhomogeneous BC may lead to various types of front reflection in a bistable system [8] and formation of complex patterns [9] or pseudo-reflection of waves [6] in the case of the oscillatory media. Wave trains were found to form in discrete excitable media that is periodically stimulated at the boundary [10].

In this paper we demonstrate that inhomogeneous BC in excitable RD systems can lead to spatiotemporal complex patterns that can be characterized as mixed-mode oscillations (see Fig. 1) with a period-adding bifurcation as a parameter is varied. This work is motivated by our experimental observation of CO catalytic oxidation over Pd supported on a glass-fiber cloth [11]. The experiments were conducted on a disk-shaped surface in a continuous reactor with feed flowing normal and through the cloth. The plate holding the catalyst was not catalytic, and its temperature was close to the ambient one. Typical infra-red (IR) thermograms exhibit mixed-mode relaxation oscillations: a hot spot expands and contracts continuously [small-amplitude fast (1 min) oscillations] superimposed on the active phase of the long duration (10–60 min) cycle (Fig. 1(a)). The number of the smaller peaks varied with operating conditions (the reactor temperature) following a period-adding mechanism [Fig. 2(a)].

A detailed mathematical model that accounts for a surface kinetic oscillator, a solid-phase enthalpy, and a gas-phase mass balance with five state variables was constructed and shown to predict two types of mixed-mode oscillations [12]. Oscillations of the first type emerge in the distributed system subject to homogeneous (no-flux) BC and completely match the solutions of the corresponding lumped model (LM, governed by ordinary differential equations). The source of such oscillations is a canard bifurcation of the reduced four-variable subsystem of the original LM, which was derived by converting one of the state variables, the solid phase temperature, to be a prescribed parameter. Oscillations of the second type emerge in the distributed system subject to in-homogeneous BC in a domain of parameters that corresponds to stable excitable steady states of the LM. These were associated with sharp front propagation and qualitatively agree with the experimental observations (Fig. 1(b)).

Our analysis will focus on the oscillations of the second type. Breathing spots have been computed and analyzed for activator-inhibitor systems [13–15], mainly in systems in which the inhibitor diffusivity is sufficiently large; it was experimentally observed in Ref. [16] and a corresponding analysis using a FitzHugh-Nagumo (FHN) bistable system subject to no-flux conditions attributed it to the interaction of the front with a boundary. Such mechanisms do not apply to catalytic systems.

The five-variable CO-oxidation model [12] can be qualitatively described by features similar to the models studied here: It is an activator-inhibitor oscillator with wide separation of time scales, coupled with an enthalpy balance which accounts for conduction and for temperature spatial distribution and boundary conditions of a fixed (cold) temperature at the catalyst's rim. Since temperature affects mainly the activator in the oscillator, we mimic it by a FHN or two-cell models with a diffusing fast activator and a slow inhibitor. Thus, the distributed FHN model, which is studied below, should capture the main features of the realistic RD system.

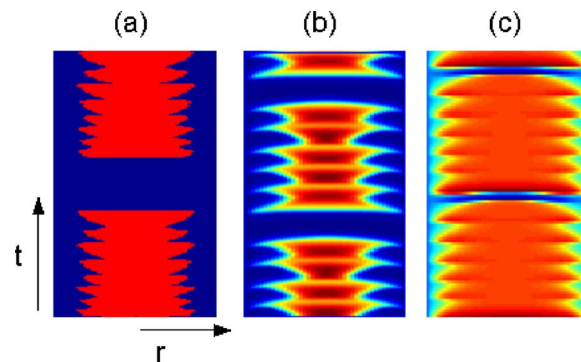To qualitatively understand the effect of BC, consider a

FIG. 1. (Color online) Typical mixed-mode oscillating patterns on a disk: (a) experiments on CO oxidation, the plate shows the square root of the active fraction of the surface [11]; (b) simulations of CO oxidation [12]; (c) x pattern simulated with the FHN model [Eqs. (5)–(7), $\alpha=0.805$; $h=100$, $x_w=-1/\sqrt{3}$, $R=10$].
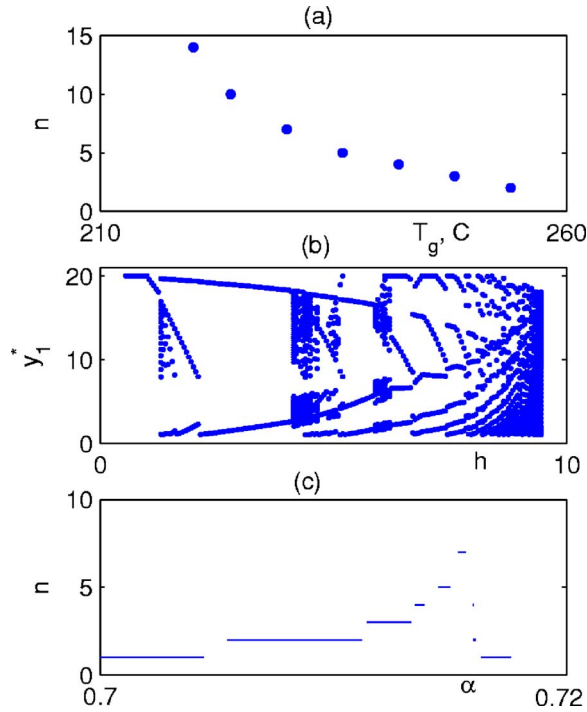
FIG. 2. (Color online) Typical bifurcation diagrams: (a) the observed number of high-frequency cycles during CO catalytic oxidation vs the reactor temperature [11]; (b) Poincaré sections of the two-cell model showing cell 1 values (y_1^*) at the switching points of cell 2 from the lower to upper branches nullcline $F_2=0$, [Eqs. (1)–(4), $a_1=-1$, $a_2=20$, $D=1$, $\alpha=12.5$, $\varepsilon \rightarrow 0$]; (c) simulations of the FHN model in a planar 1D system [Eqs. (5)–(7), $L=160$, $h=100$, $x_w=-1/\sqrt{3}$, $\varepsilon=0.1$]

lumped many-cell version of the distributed model assuming that all cells with the exception of the last one are excitable, in the absence of interaction, while the last (boundary) one is stable but belongs to the null-cline branch opposite of the fixed point of the excitable cells. The interaction of adjacent cells causes gradual shifting of each "individual" cell phase plane starting from the edge one and will produce for one or more cells conditions that induce an oscillatory behavior. The chain interaction of the following cells can induce the temporally mixed-mode oscillations. Thus, the simplest prototype to yield the expected behavior is a pair of coupled excitable and oscillatory cells. This is similar to previous studies of an excitable cell that is periodically stimulated by a fixed external force and was shown to exhibit a period-adding scenario [17]. Here the oscillatory forcing system is coupled to the excitable one.

The spatial pattern is achieved by motion of fronts or pulses in the excitable media. As will be shown below, all three models exhibit period-adding bifurcation with varying a parameter that defines the effect of the boundary conditions.

Pair of coupled and excitable and oscillatory cells. We assume that cell 1 is excitable, while cell 2 is oscillatory and is affected by the same factors as those of cell 1, as well as by an external force $F=h(x-x_w)$ that mimics the BC. The spontaneous dynamics of both cells is governed by a caricature of the FHN model with a piecewise linear nonlinearity
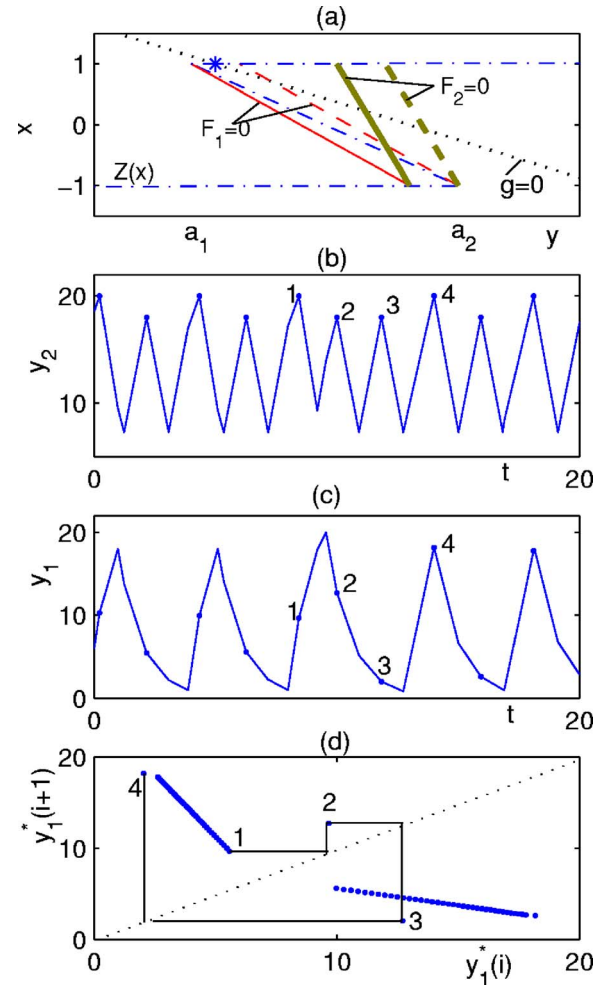

FIG. 3. (Color online) Coupled cells model [Eqs. (1)–(4)]. Plate (a) shows a phase plane with nullcline $g(x,y)=0$ (dotted line), source function $Z(x)$ (dash-dotted) and the intermediate branches of nullclines $F_i(x_i,y_i)=0$ of cells 1 (thin) and 2 (thick lines), respectively. Solid and dashed lines F_i for each cell are calculated with an assumption that the other cell belongs to the upper (solid) and lower (dashed) branches, respectively. The star marks a fixed point of the isolated cell. Plates (b) and (c) show fragments of the temporal profiles $y_2(t)$ and $y_1(t)$ of $P_1^3(P_1^2)^{38}$ solution in the vicinity of the "defect" oscillation P_1^3. Plate (d) presents a return map constructed by Poincaré section showing y_1 values [y_1^*, points in (c)] at times corresponding to local maxima in $y_2(t)$ [points in (b)].

$$\dot{x}_1 = y_1 - Z(x_1) - D(x_1 - x_2) = F_1(x_i, y_1), \qquad (1)$$

$$\dot{x}_2 = y_2 - Z(x_2) + D(x_1 - x_2) - h(x_2 - x_w) = F_2(x_i, y_2), \quad (2)$$

$$\dot{y}_i = \varepsilon(-\alpha(x_i - 1) - y_i) = g(x_i, y_i), \quad i = 1, 2, \qquad (3)$$

$$Z(x) = \begin{cases} a_2 + (x+1)/\gamma, & x \in (-\infty, -1], \\ a_2 - 0.5(a_2 - a_1)(x+1), & x \in (-1, 1), \\ a_1 + (x-1)/\gamma, & x \in [1, \infty), \end{cases} \qquad (4)$$

with $\varepsilon, \gamma \ll 1$. We assume that the fixed point of a single isolated cell x_s (with $D=h=0$) is excitable and x_w belongs to the branch opposite of x_s [Fig. 3(a)]. Keeping in mind that ε,

$\gamma \ll 1$ while a_1, $a_2 \sim O(1)$, the dynamics of each cell can be described by a binary model with $x_i \simeq +1$ or -1 along the upper or lower branches $Z(x)$, respectively. We can construct phase planes of each cell, assuming that the other cell moves along one of the stable branches of the corresponding null curve. The limit points of the phase plane of cell 1 coincide with the limit points of function $Z(x)$ if both cells move along the same branch and are shifted by $2D$ if the cells belong to the opposite branches. The limit points of the phase plane of cell 2 get additional shifting at the upper branch by $2h$ due to the external forcing. Simple geometrical consideration allows derivation of the following conditions for cell 1 to be excitable and cell 2 to be oscillatory: $y_s - a_1 < 2h < a_2 - a_1 - 2D$, $y_s - a_1 < 2D < a_2 - a_1 - 2h$.

Analysis of system (1)–(4) even in the case of a binary model ($\varepsilon \to 0$), is rather cumbersome: we can define up to three and four different close orbits based on various sets of limit points for cells 1 and 2 while a continuous spectrum is expected within these intervals.

A typical numerically calculated bifurcation diagram of the binary model is presented in Fig. 2(b). It is constructed by Poincaré sections showing y_1 values at times corresponding to cell 2 switching from the lower to upper branch of null-curve $F_2 = 0$ [at local maxima $y_2(t)$]. The bifurcation diagram exhibits domains of regular P_1^n solutions (one oscillation of the excitable cell is coupled with n oscillations of the oscillatory cell). And we detected two types (I, II, see Ref. [18]) of period-adding bifurcations. For example, for a set of parameters used in Fig. 2(b) we found windows of chaotic behavior between domains P_1^2 and P_1^3, or P_1^6 and P_1^7, etc., while transitions $P_1^4 \to P_1^5$ and $P_1^5 \to P_1^6$ occur without any intermediate states (up to resolution of 10^{-4} in h). A complex $P_1^3 (P_1^2)^{38}$ solution (i.e., a cycle is composed of one P_1^3 oscillation coupled with 38 oscillations of P_1^2 type) is illustrated by Figs. 3(b) and 3(c). The corresponding return map [Fig. 3(d)] constructed by the Poincaré section [Fig. 2(b)] exhibits two separate branches with negative slopes and several isolated points corresponding to the system behavior in the vicinity of the "defect" oscillation P_1^3. With increasing complexity of the solution the corresponding return map becomes more complex as well, e.g., for a $(P_1^3 P_1^4)^4 P_1^4$ solution ($h = 6.1$, within transition $P_1^3 \to P_1^4$) the return map is composed of five separated branches of different slopes. This is in principal difference with the single periodically stimulated excitable cell [17], which does not exhibit chaotic response.

In the case of finite ε the limit solutions considered above can be referred to as *outer* solutions (following Ref. [17]) and we expect to find some new bifurcation structures. The detailed analysis of this problem is beyond the scope of the present paper.

Distributed FitzHugh-Nagumo system. We employ a simple model with a fast distributed activator, and a local slow inhibitor

$$\dot{x} - \Delta x = -x^3 + x + y = f(x, y), \qquad (5)$$

$$\dot{y} = \varepsilon(-\alpha x - y + \beta) = g(x, y) \qquad (6)$$

subject to the following boundary conditions:
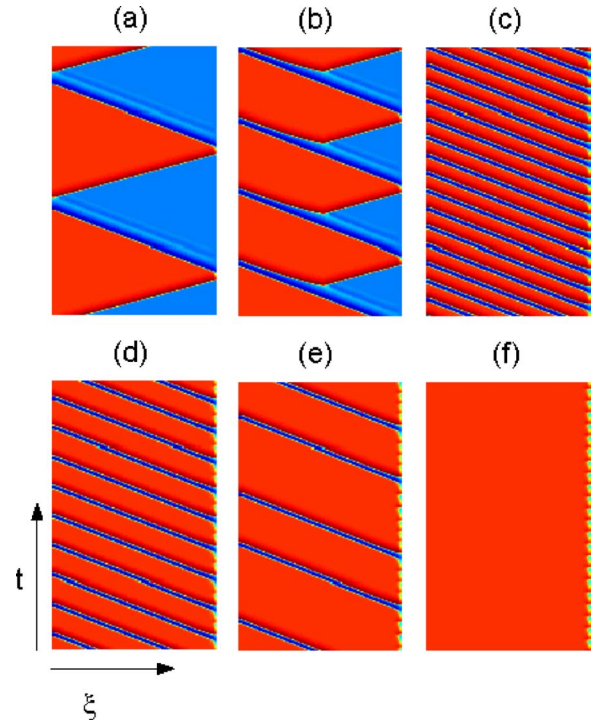

FIG. 4. (Color online) Typical bifurcation sequence of spatiotemporal x pattern of the FHN model [Eqs. (5)–(7)] with varying parameter α in a long system: (a) back-and-force pulse ($\alpha = 0.59$), (b) periodic traveling pulses with a source point (0.590 25); moving pulses of P_1^1 (0.70, c), P_1^2 (0.710, d), $P_1^5 P_1^7$ (0.713, e) types, and a quasi-stationary pattern with a period-one small amplitude oscillations (0.715, f), $\varepsilon = 0.1$, $h = 100$, $x_w = -1/\sqrt{3}$.

$$\xi = 0: \partial x / \partial \xi = 0, \quad \xi = L: \partial x / \partial \xi = h(x - x_w), \qquad (7)$$

where ξ denotes the spatial or radial coordinate in a planar case or in a disk, respectively. The diffusion coefficient (D) is set to unity in Eq. (5) after rescaling the length with respect to $\sqrt{D}$, while the dimensionless system length is L. We keep the steady state solution (SS) fixed at x_s^+ (=0.7) and vary parameters α (β is adjusted to keep the SS), x_w (always negative) and h. For such a choice the lumped system possesses three SS solutions ($x_s^\pm$ and x^0) when $\alpha \leq \alpha_1 \simeq 0.6325$ and a single steady state when $\alpha > \alpha_1$. The x_s^+ state is excitable, x^0 is a saddle point and x_s^- admits a Hopf bifurcation at $\alpha_H = 1 - (x_s^+)^2 - (x_H)^2 - x_s^+ x_H \simeq 0.5933$ with $x_H = -\sqrt{(1 - \varepsilon)/3}$.

Numerical simulations of one-dimensional (1D) Cartesian system revealed that the stationary quasi-homogeneous solution (with $x(\xi) \in [x_s^-, x_w]$) bifurcates to moving patterns at a certain threshold value α^* around α_H. The sustained pattern [Fig. 4(a)] exhibits a narrow front separating domains with $x = x_s^+$ and $x = x_s^-$, that is bouncing from both boundaries. For $\alpha > \alpha^*$ we detected four subdomains of different system behavior: (i) patterns with a source point [SP, Fig. 4(b)]; (ii) simple wave trains [Fig. 4(c)]; (iii) traveling pulses of complex structure with period-adding bifurcations (Figs. 4(d) and 4(e) and Fig. 1(c); (iv) a quasi-stationary solution with $x(\xi) = x_s^+$ for most part of the region and small amplitude spatiotemporal oscillations near the boundary

$\xi=L$ [Fig. 4(f)]. Just above that domain the system exhibits a stationary solution.

Let us focus on the system behavior within subdomain (iii). The state variables exhibit small-amplitude temporal oscillations in the vicinity of the right boundary which admit period-adding bifurcations with varying any of the parameters: α, h, x_w. Some of these oscillations will induce a traveling pulse that moves through most parts of the computational domain. The spatial period can be estimated by the velocity and the global period of the temporal oscillations. Domains of regular P_1^n solutions were always found to be alternated by windows of chaotic behavior but we did not detect any regular tendency of the staircase structure. For a set of parameters employed in Fig. 2(c) we found a domain of $P_1^5 P_1^7$ solution [Fig. 4(e)], while a stable P_1^6 was not observed.

The boundaries of the detected subdomains ($i-iv$ above) depend on the system parameters: they are shifted toward lower α values with increasing x_w or decreasing h, i.e., with weakening the impact of BC. We will briefly list several essential features of sustained patterns within the other subdomains: In subdomain (i) two opposite propagating ignition fronts are born at the source point (SP) within the computational domain. The left front leaves the system (no-flux BC) while the right front is reflected from $\xi=L$ boundary. With increasing α the SP moves from the left boundary (at α^*) toward $\xi=L$. Within subdomain (iv) with decreasing α the system exhibits a sequence of period-doubling bifurcations which switch to chaotic behavior and terminate at the critical point.

Numerical two-dimensional simulations on a disk revealed only axisymmetric patterns. For sufficiently large R these patterns admit with varying a parameter the same bifurcation sequence which was detected for a planar case and the boundaries of the subdomains practically coincide with those of the 1D system. With decreasing R, the domain of complex patterns is shifted (particularly, toward largest α). For relatively small R the moving train solution can be "arrested" and, moreover, the direction of the front propagation can be changed (the similar tendency was revealed in a planar system of small L). The observed patterns are of the form of breathing motion [Fig. 1(c)]. Such patterns are in a good qualitative agreement with our experimental results and numerical simulations of pattern states during CO catalytic oxidation [12].

In summary we showed that inhomogeneous BC in distributed excitable media can induce moving pulses. The bifurcation structure can be described as period adding separated by windows of chaotic behavior. The proposed mechanism allows one to explain experimentally observed patterns during catalytic CO oxidation. Similar mechanisms can be applied for many other systems.

[1] J. D. Murray, *Mathematical Biology* (Springer, Berlin, 1989).

[2] E. Meron, Phys. Rep. **218**, 1 (1992).

[3] M. C. Cross and P. C. Hohenberg, Rev. Mod. Phys. **65**, 851 (1993).

[4] M. Or, I. G. Kevrekidis, and M. Bär, Physica D **135**, 154 (2000).

[5] D. Luss and M. Sheintuch, Catal. Today **105**, 254 (2005).

[6] A. Rabinovitch, M. Gutman, and I. Aviram, Phys. Rev. E **67**, 036212 (2003); **70**, 037202 (2004).

[7] J. Kosek and M. Marek, Phys. Rev. Lett. **74**, 2134 (1995).

[8] A. Yadav and D. A. Browne, Phys. Rev. E **70**, 036218 (2004).

[9] S. Bouzat and H. S. Wio, Physica A **317**, 472 (2003).

[10] A. Carpio, Physica D **207**, 117 (2005).

[11] R. Digilov, O. Nekhamkina, and M. Sheintuch, AIChE J. **50**, 163 (2004).

[12] O. Nekhamkina, R. Digilov, and M. Sheintuch, J. Chem. Phys. **119**, 2322 (2003); *Eighth Experimental Chaos Conference*, AIP Conf. Proc. No. 742 (AIP, New York, 2004), pp. 15–20.

[13] D. Haim, G. Li, Q. Ouyang, W. D. McCormick, H. L. Swinney, A. Hagberg, and E. Meron, Phys. Rev. Lett. **77**, 190 (1996).

[14] S. Koga and Y. Kuramoto, Prog. Theor. Phys. **63**, 106 (1980); Y. Nishiura and M. Mimura, SIAM J. Appl. Math. **49**, 481 (1989); B. S. Kerner and V. V. Osipov, Sov. Phys. Usp. **32**, 101 (1989); U. Middya, D. Luss, and M. Sheintuch, J. Chem. Phys. **100**, 3568 (1994).

[15] A. Hagberg and E. Meron, Nonlinearity **7**, 805 (1994).

[16] V. Gáspár and K. Showalter, J. Am. Chem. Soc. **109**, 4869 (1987).

[17] S. Coombes and A. H. Osbaldestin, Phys. Rev. E **62**, 4057 (2000).

[18] A. V. Holden and Y. S. Fan, Chaos, Solitons Fractals **2**, 221 (1992); **3**, 439 (1993).